Numerical experiments on the determination of stress concentration factors in orthotropic perforated plates subjected to in – plane loading

D.V. Bambill, C.A. Rossit† and A. Susca

Dpto. de Ingeniería-Instituto de Mecánica Aplicada-Universidad Nacional del Sur–(8000) Bahía Blanca-Argentina
Consejo Nacional de Investigaciones Científicas y Técnicas-CONICET, Argentina

(Received March 27, 2008, Accepted May 23, 2009)

Abstract. As it is known, laminated composite materials are increasingly used in many technological applications, and in some instance, cutouts must be made into laminated panels for practical reasons, changing the stress distribution. The present study deals with the determination of the stress concentration factor that holes of square shape cause in an orthotropic plate subjected to distributed in – plane loading. Square holes of rounded corners in a rectangular plate are considered, and the effect of different combinations of axial and tangential forces applied to its middle plane at the external edges, is studied. The mutually perpendicular axes, which define the principal axes of orthotropy, are assumed in many different directions referred to the sides of the plate. Numerical experiments by means of a finite element code is performed, evaluating the influence of the fiber orientation with respect to the edges of the plate and the characteristics of the orthotropic materials since such structures do not exhibit easily predictable behavior.

Keywords: stress concentration; S.C.F.; orthotropic plates; plane stress; finite element method.

1. Introduction

Scientific and technological requirements have incremented the need of use of new materials and in some cases rather "unbelievable" constitutive parameters are attained[1].

Orthotropic materials constitute a rather simple but common situation in modern technology where composite materials are increasingly used. Moreover metals as steel, aluminium, etc., can acquire orthotropic characteristics due to the manufacturing procedures.

In some cases, different cutout shapes in thin panels are performed to provide access to other parts of the structure, passage of ducts or electrical cables, etc.

It is known that the presence of a cutout in a stressed member creates highly localized stresses around the hole, the ratio of the maximum stress at the hole edge to the nominal stress of the solid

[1]This is the case, for instance, of auxetic materials (used in bioengineering applications) where Poisson's ratio is negative.

† Ph.D., Corresponding author, E-mail: carossit@criba.edu.ar

plate is called stress concentration factor (S.C.F.).

A paradigmatic case in the field was solved by Kirsch (1898) over one hundred years ago, for isotropic plates.

Design engineers can find a great amount of information in the open literature on stress concentration factor in isotropic plates (Pilkey 1997), but there is a rather limited amount in the case of orthotropic plates with holes, and in general mainly referred to infinite plates.

Lekhnitskii (1968) has developed an analytic approach for the subject matter and obtained a limited amount of data.

Additional analytical studies have been developed later on.

Among them one can mention the following papers:

Hufenbach *et al.* (1990) obtained an analytical solution for stress and displacement field around an elliptical hole in an anisotropic plate. Ukadgaonker and Awasare (1994) used the superposition principle to obtain explicit mathematical solutions for various regular shapes of holes.

Wu and Mu (2003) investigated the SCF for orthotropic cylindrical shells with circular cutout.

As it is an important subject in Mining Engineering, it is worthwhile of mentioned the papers of Park and Kim (2006) and Sharan (2007).

In general, numerical (Hüsnü and Alaattin 2000, Rezaeepazhand and Jafari 2005, Susca *et al* 2006, Shrestha and Ohga 2006) or experimental techniques (Amer and Schadler 1997, Toubal *et al.* 2005) must be used in order to determine SCF in composite plates.

In this paper a general approach is used to analyze a rectangular plate made of an orthotropic material with a small square hole with rounded corners subjected to in-plane axial and tangential loading applied at the edges. The orientations of the constitutive axes 1 and 2 were varied with respect to the plate sides and loading directions. These relative positions are denoted with the angle θ (Fig. 1).

The geometry of the cutout is illustrated in Fig. 2. The calculations have been performed using a well-known finite element code (Algor 2007) and exhibit excellent agreement for particular cases with the analytical solution proposed by Lekhnitskii (1968).

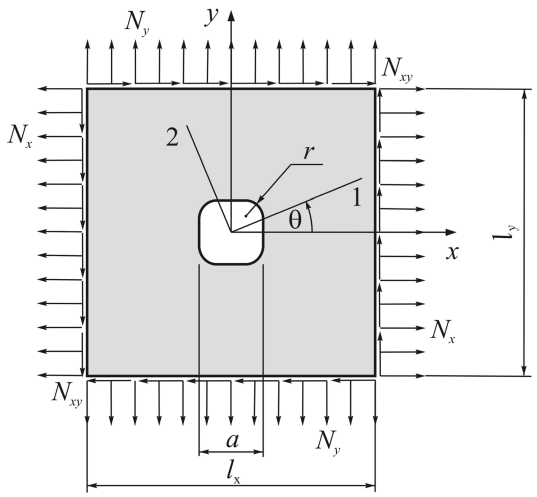

Fig. 1 System under consideration

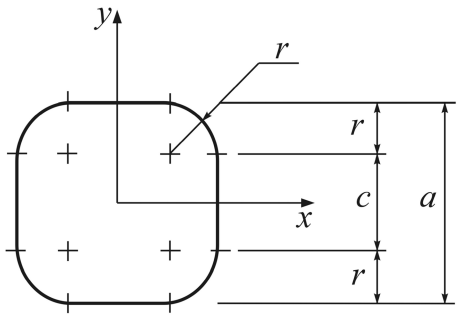

Fig. 2 Square hole with rounded corners considered: $r/a = 0.22$, $c/a = 0.56$

2. Basic theoretical formulation

As it is well known, in the case of plane state of stress and in the absence of body forces, (Maiz *et al.* 2004), the problem in Cartesian coordinates x, y, is governed by:

a) Equilibrium equations

$$\frac{\partial \sigma_x}{\partial x} + \frac{\partial \tau_{xy}}{\partial y} = 0 \tag{1a}$$

$$\frac{\partial \tau_{xy}}{\partial x} + \frac{\partial \sigma_y}{\partial y} = 0 \tag{1b}$$

where σ_x, σ_y are the normal components and $\tau_{xy} = \tau_{yx}$ are the shear components of the stress tensor.

b) Constitutive equations

When the elasticity axes coincide with the coordinate axes ($\theta = 0$)

$$\varepsilon_x = \frac{\sigma_x}{E_1} - \nu_2 \frac{\sigma_Y}{E_2} = \frac{1}{E_1}(\sigma_x - \nu_1 \sigma_y) \tag{2a}$$

$$\varepsilon_y = \frac{\sigma_y}{E_2} - \nu_1 \frac{\sigma_X}{E_1} = \frac{1}{E_2}(\sigma_Y - \nu_2 \sigma_X) \tag{2b}$$

$$\gamma_{XY} = \frac{\tau_{XY}}{G_{12}} \tag{2c}$$

where E_1, E_2 are the corresponding Young's moduli along the principal directions of elasticity 1 and 2, ν_1, ν_2 are the Poisson's ratios; G_{12} is the shear modulus and $\varepsilon_x, \varepsilon_y, \gamma_{xy}$ are the strains in the Cartesian system.

The following relation between the Young's moduli and the Poisson ratios exists: $\nu_1/E_1 = \nu_2/E_2$ due to the symmetry of Eq. (2).

Obviously, when the directions of elasticity 1, 2 do not coincide with the directions x, y, expressions (2) are more complicated.

c) Strain - Displacement relations

$$\varepsilon_x = \frac{\partial u}{\partial x}; \quad \varepsilon_y = \frac{\partial v}{\partial y}; \quad \gamma_{xy} = \frac{\partial v}{\partial x} + \frac{\partial u}{\partial y} \tag{3a,b,c}$$

where u, v are the displacements in directions x, y.

d) Compatibility condition

$$\frac{\partial^2 \gamma_{xy}}{\partial x \partial y} = \frac{\partial^2 \varepsilon_x}{\partial y^2} + \frac{\partial^2 \varepsilon_y}{\partial x^2} \tag{4}$$

Substituting Eq. (2) in Eq. (4) yields the compatibility equation in terms of the components of the stress tensor.

$$\frac{1}{G_{12}}\frac{\partial^2 \tau_{xy}}{\partial x \partial y} = \frac{1}{E_1}\left(\frac{\partial^2 \sigma_x}{\partial x^2} - \nu_1 \frac{\partial^2 \sigma_x}{\partial x^2}\right) + \frac{1}{E_2}\left(\frac{\partial^2 \sigma_y}{\partial x^2} - \nu_2 \frac{\partial^2 \sigma_y}{\partial y^2}\right) \tag{5}$$

Finally, the calculated stresses and/or displacements must satisfy the prescribed boundary conditions.

3. Finite element modeling

A commercial finite element code, available for every designer, was used to perform the numerical experiments presented in this paper.

As it is known, an important point in the process of obtaining accurate values is the design of the mesh of the elements.

In order to optimize the mesh design, the fulfillment of the boundary condition was chosen as optimization parameter, particularly the null value of the normal component stress perpendicular to the edge of the hole.

Quadrangular and triangular conformal elements with four and three nodes respectively are combined. Those elements possess two degrees of freedom at each node and are suitable for the plane stress problem.

Trial runs were made to select the proper net of finite elements for each problem.

As a general rule, obviously the density of the mesh is strongly increased in the proximities of the cutout where stress gradient is higher.

In particular around the corners, concentric circumferences and radial lines construct quadrangular elements.

The distance between circumferences increases gradually with the ratio in order to obtain trapeziums of regular shape.

The density of elements diminishes towards the center of the sides of the rectangle where the stress gradient is lower. The transition was made with three node elements.

Far away from the hole, the stress field is not affected significatively, so the mesh density decreases strongly.

Fig. 3 shows schematically the selected mesh for the problem.

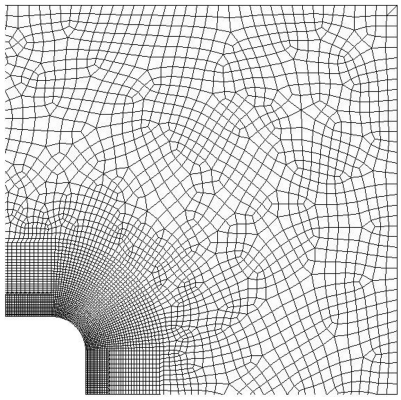

Fig. 3 Mesh details near the edge of the hole

4. Numerical and graphical results

The procedure was verified comparing for the analytical approximated solution proposed by Lekhnitskii (1968). He considered a rectangular infinite orthotropic plate with the principle directions of elasticity parallel to its sides.

The plate is weakened at its center by a small opening, the contour of which is described by the parametric equation

$$\begin{aligned} x &= r[\cos(\alpha) + \varepsilon\cos(m\alpha)] \\ y &= r[c\sin(\alpha) - \varepsilon\sin(m\alpha)] \end{aligned} \tag{6}$$

where axes x and y are parallel to the sides, $0 < c \leq 1$ and m is an integer.

For certain values of the parameters included, the opening differs slightly from a square with rounded corners.

Lekhnitskii solved the problem for a square hole $[m = 3, c = 1, \varepsilon = -1/9]$ in an orthotropic plate subjected to tension by forces p which are uniformly distributed on two opposite sides (Fig. 4).

The orthotropic material chosen by Lekhnitskii is defined by:

$$E_1 = 1.2\ 10^5 \frac{\text{kg}}{\text{cm}^2}; \quad E_2 = 0.6\ 10^5 \frac{\text{kg}}{\text{cm}^2}; \quad G_{12} = 0.07\ 10^5 \frac{\text{kg}}{\text{cm}^2}; \quad \nu_1 = 0.071$$

He studied cases both of tension in direction of the largest Young's modulus ($E_x = E_{\max}$) and the smallest ($E_x = E_{\min}$) respectively.

In Table 1 a comparison is made with the results obtained in the present study.

Table 1 Stress concentration factors at contour points of a square opening in an orthotropic plate under axial tension

Point	$E_x = E_{máx}$		$E_x = E_{min}$	
	Lekhnitskii	Present Study	Lekhnitskii	Present Study
A	$-0.57\,p$	$-0.58\,p$	$-1.11\,p$	$-1.11\,p$
B	$2.60\,p$	$2.57\,p$	$2.22\,p$	$2.21\,p$
C	$0.83\,p$	$0.71\,p$	$1.28\,p$	$1.11\,p$

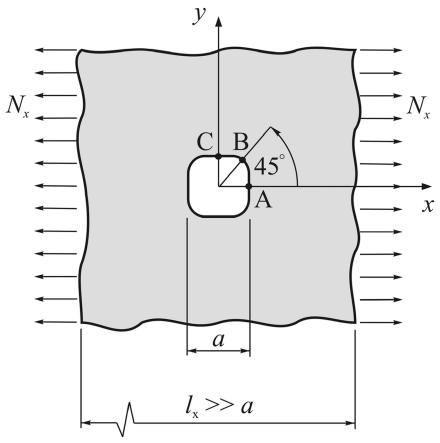

Fig. 4 Infinite orthotropic plate under uniaxial tension studied by Lekhnitskii

A, B and C are selected points at the contour of the hole (Fig. 4).

Previously, numerical experiments have been performed in order to find out the hole size to plate dimensions ratio (a/l) up to which the stress distribution is not affected and the plate may be considered infinite. That ratio was found to be: $a/l = 0.005$.

A very good agreement is observed, for points A and B. At point C the difference obey to the fact that the constant curvature of the model under study at the cutout corners differs from the geometry that arises from Eq. (6) in the neighborhood of the corners.

Once the procedure was checked-up, numerical and graphical results were obtained.

In the first place, the case of a square plate of graphite-epoxy, with a centered square hole with rounded corners subjected to general, in - plane loading is studied.

The elastic parameters of material considered are:

$$E_1 = 181 \text{ GPa}; \quad E_2 = 10.3 \text{ GPa}; \quad G_{12} = 7.77 \text{ GPa}; \quad \nu_1 = 0.28; \quad \nu_2 = 0.01593$$

The orientations of the constitutive axes 1, and 2, were varied with respect to the plate sides and loading direction (which is taken coincident with the Cartesian axe: x).

Accordingly, the following values of θ were taken: 0º, 22,5º, 45º, 67,5º, 90º.

The concentration factors calculated were conveniently defined as:

$$K_+ = \frac{\sigma_{\max}}{\sigma_n}; \quad K_- = \frac{\sigma_{\min}}{\sigma_n}$$

where σ_n is the principal stress of the solid plate, at the point of the contour where $\sigma_{\max}$ or $\sigma_{\min}$ occurs.

Table 2 S.C.F for a perforated square plate subjected to different combinations of external forces and orientation of elastic axes (graphite/epoxy). $a/l = 0.2$

$a/l = 0.2$		θ^o				
		-45	-22,5	0	22,5	45
$\frac{N_{xy}}{N} = 1$	K_+	3,67	5,09	10,99	13,04	14,07
	β_+	135,36	120,09	121,45	128,41	135,00
	K_-	-7,86	-7,17	-6,00	-1,63	-0,50
	β_-	45,00	51,76	59,06	60,25	45,00
$\frac{N_{xy}}{N} = 0,75$	K_+	3,6	4,85	10,14	12,01	12,95
	β_+	135,36	135,36	121,45	128,41	135,00
	K_-	-5,85	-5,31	-4,45	-0,91	-
	β_-	45,00	45,00	59,06	60,42	-
$\frac{N_{xy}}{N} = 0,5$	K_+	3,51	4,55	9,01	10,65	11,45
	β_+	135,36	135,36	121,62	128,41	135,00
	K_-	-3,17	-2,83	-2,42	-0,31	-
	β_-	45,00	45,00	59,57	96,04	-
$\frac{N_{xy}}{N} = 0,25$	K_+	3,37	4,12	7,45	8,74	9,35
	β_+	135,36	120,09	121,79	128,41	135,00
	K_-	-	-	-0,48	-	-
	β_-	-	-	72,07	-	-
$\frac{N_{xy}}{N} = 0$	K_+	6,22	5,87	5,14	5,87	6,22
	β_+	45,00	52,65	57,87	127,36	135,00
	K_-	-	-	-0,22	-	-
	β_-	-	-	90,00	-	-

Table 3 S.C.F for a perforated square plate subjected to different combinations of external forces and orientation of elastic axes (graphite/epoxy). $a/l = 0.1$

$a/l = 0.1$		θ^o				
		-45	-22,5	0	22,5	45
$\frac{N_{xy}}{N} = 1$	K_+	3,33	4,62	9,34	10,74	11,28
	β_+	135,36	120,09	121,62	128,41	135,00
	K_-	-5,45	-5,22	-4,95	-1,35	-0,34
	β_-	45,00	51,76	59,06	60,25	45,00
$\frac{N_{xy}}{N} = 0,75$	K_+	3,28	4,43	8,65	9,99	10,50
	β_+	135,36	120,09	121,62	128,41	135,00
	K_-	-3,84	-3,69	-3,65	-0,70	-
	β_-	45,00	51,76	59,23	60,42	-
$\frac{N_{xy}}{N} = 0,5$	K_+	3,22	4,17	7,73	9,00	9,46
	β_+	135,36	120,09	121,79	128,41	135,00
	K_-	-1,69	-1,65	-1,96	-0,29	-
	β_-	45,00	51,94	59,74	99,54	-
$\frac{N_{xy}}{N} = 0,25$	K_+	3,13	3,82	6,46	7,61	8,01
	β_+	135,36	120,26	121,96	128,41	135,00
	K_-	-	-	-0,56	-	-
	β_-	-	-	73,37	-	-
$\frac{N_{xy}}{N} = 0$	K_+	5,82	5,52	4,61	5,52	5,82
	β_+	45,00	51,41	57,52	128,59	135,00
	K_-	-	-	-0,40	-	-
	β_-	-	-	90,00	-	-

Table 4 S.C.F for a perforated square plate subjected to different combinations of external forces and orientation of elastic axes (graphite/epoxy). $a/l = 0.05$

$a/l = 0.05$		θ^o				
		-45	-22,5	0	22,5	45
$\frac{N_{xy}}{N} = 1$	K_+	3,27	4,50	8,92	10,05	10,64
	β_+	135,36	120,09	121,62	128,41	135,00
	K_-	-4,84	-4,63	-4,64	-1,27	-0,31
	β_-	45,00	51,76	59,06	60,25	45,00
$\frac{N_{xy}}{N} = 0,75$	K_+	3,22	4,32	8,27	9,39	9,95
	β_+	135,36	120,09	121,79	121,41	135,00
	K_-	-3,32	-3,20	-3,40	-0,63	-
	β_-	45,00	51,76	59,29	60,42	-
$\frac{N_{xy}}{N} = 0,5$	K_+	3,17	4,08	7,41	8,51	9,02
	β_+	135,36	120,09	121,79	128,41	135,00
	K_-	-1,30	-1,29	-1,80	-0,28	-
	β_-	45,00	51,94	59,74	100,92	-
$\frac{N_{xy}}{N} = 0,25$	K_+	3,08	3,74	6,23	7,27	7,73
	β_+	135,36	120,26	121,96	128,41	135,00
	K_-	-	-	-0,56	-	-
	β_-	-	-	74,03	-	-
$\frac{N_{xy}}{N} = 0$	K_+	5,79	5,43	4,51	5,43	5,80
	β_+	45,00	51,41	57,35	128,59	135,00
	K_-	-	-	-0,43	-	-
	β_-	-	-	90,00	-	-

Table 5 S.C.F for a perforated square plate subjected to different combinations of external forces and orientation of elastic axes (graphite/epoxy). $a/l = 0.01$

$a/l = 0.01$		θ^o				
		-45	-22,5	0	22,5	45
$\frac{N_{xy}}{N} = 1$	K_+	3,24	4,45	8,75	9,76	10,38
	β_+	135,36	120,09	121,62	128,41	135,00
	K_-	-4,59	-4,39	-4,54	-1,24	-0,29
	β_-	45,00	51,76	59,06	60,25	45,00
$\frac{N_{xy}}{N} = 0,75$	K_+	3,20	4,27	8,13	9,14	9,72
	β_+	135,36	120,09	121,79	128,41	135,00
	K_-	-3,11	-2,99	-3,32	-0,61	-
	β_-	45,00	51,76	59,23	60,58	-
$\frac{N_{xy}}{N} = 0,5$	K_+	3,15	4,04	7,29	8,30	8,84
	β_+	135,36	120,09	121,79	128,41	135,00
	K_-	-1,14	-1,14	-1,75	-0,28	-
	β_-	45,00	51,94	51,91	101,60	-
$\frac{N_{xy}}{N} = 0,25$	K_+	3,07	3,72	6,14	7,13	7,61
	β_+	135,36	120,26	121,96	128,59	135,00
	K_-	-	-	-0,57	-	-
	β_-	-	-	74,36	-	-
$\frac{N_{xy}}{N} = 0$	K_+	5,77	5,38	4,47	5,39	5,77
	β_+	45,00	51,41	57,35	128,59	135,00
	K_-	-	-	-0,44	-	-
	β_-	-	-	90,00	-	-

Table 6 S.C.F for a perforated square plate subjected to different combinations of external forces and orientation of elastic axes (graphite/epoxy). $a/l = 0.005$

$a/l = 0.005$		θ^o				
		-45	-22,5	0	22,5	45
$\frac{N_{xy}}{N} = 1$	K_+	3,24	4,45	8,74	9,72	10,29
	β_+	135,36	120,09	121,62	128,41	135,00
	K_-	-4,53	-4,34	-4,50	-1,23	-0,28
	β_-	45,00	51,76	59,06	60,25	45,00
$\frac{N_{xy}}{N} = 0,75$	K_+	3,20	4,27	8,11	9,10	9,65
	β_+	135,36	120,09	121,79	90,79	135,00
	K_-	-3,06	-2,96	-3,29	-0,60	-
	β_-	45,00	51,76	59,23	60,58	-
$\frac{N_{xy}}{N} = 0,5$	K_+	3,14	4,04	7,28	8,27	8,78
	β_+	135,36	120,09	121,79	128,41	135,00
	K_-	-1,10	-1,11	-1,73	-0,28	-
	β_-	45,00	51,94	59,91	101,60	-
$\frac{N_{xy}}{N} = 0,25$	K_+	3,07	3,71	6,13	7,11	7,58
	β_+	135,36	120,26	121,96	128,59	135,00
	K_-	-	-	-0,57	-	-
	β_-	-	-	74,36	-	-
$\frac{N_{xy}}{N} = 0$	K_+	5,77	5,38	4,46	5,37	5,76
	β_+	45,00	128,59	122,65	128,59	135,00
	K_-	-	-	-0,45	-	-
	β_-	-	-	90,00	-	-

The case of $N_x = N_y = N$ and different values of N_{xy}/N = 0, 0.25, 0.5, 0.75, and 1 are taken.

Values of K_+ and K_- are depicted in Tables 2 to 6, for plates of different *a/l* ratios.

The Tables contain also the values of β_+ and β_-, where β_+ defines the azimuthal value of hole contour coordinate where the maximum tensile stress takes place and β_- corresponds the maximum compressive stress[2]. When there is no compression, the value of K_- is omitted.

Obviously, compressive stresses increase with the relative magnitude of N_{xy}.

One observes that when the ratio *a/l* decreases the obtained values tend to be constant

Fig. 5 to 8 make evident this behavior for particular cases of the system under study. The relation between hole and plate sizes is expressed as *l/a* in those Figures in order to emphasize the asymptotic behavior of the obtained parameters as the hole size decreases.

Furthermore, Figs. 5 and 6 show the variation of K_+, for different sizes of the hole and kinds of loads, and two particular orientations of the constitutive axes ($\theta = -45^\circ$ and 45° respectively).

Meanwhile Figs. 7 and 8 show the variation of K_+ for different sizes of the hole and orientations of the elastic axes, and two particular situation of the in-plane loading ($N_{xy}/N = 1$ respectively).

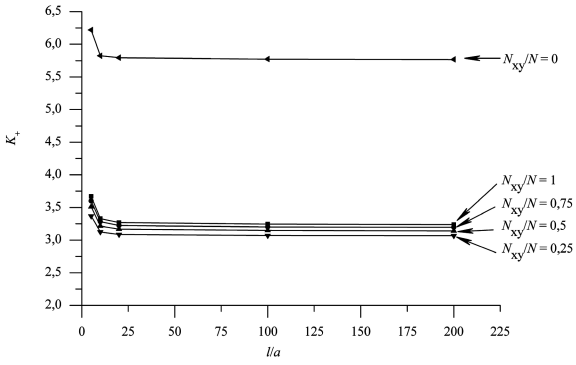

Fig. 5 K_+ vs. *l/a* curves for different values of N_{xy}/N and $\theta = -45^\circ$

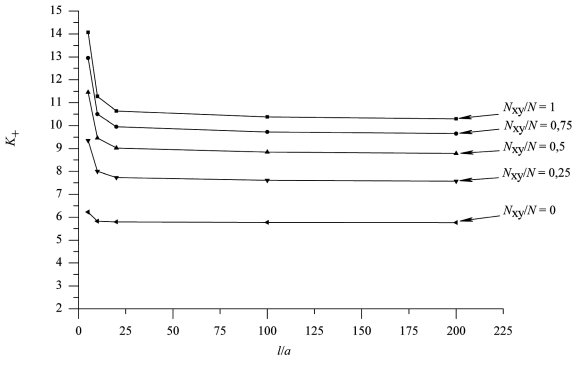

Fig. 6 K_+ vs. *l/a* curves for different values of N_{xy}/N and $\theta = 45^\circ$

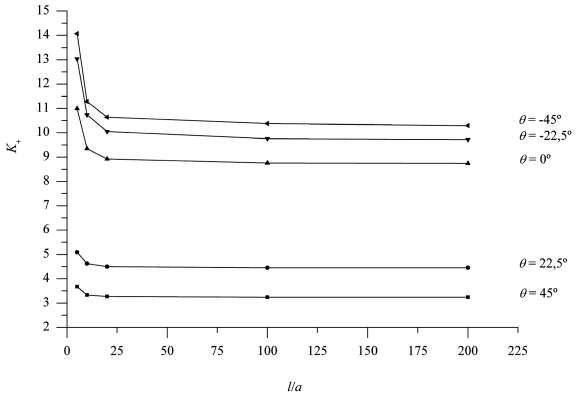

Fig. 7 K_+ vs. *l/a* curves for different orientation of elastic axes, θ, and $N_{xy}/N = 1$

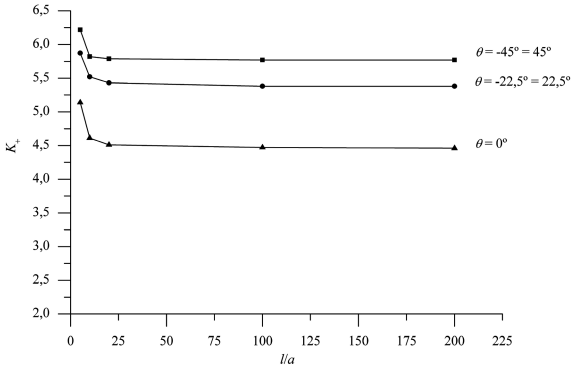

Fig. 8 K_+ vs. *l/a* curves for different orientation of elastic axes, θ, and no shear forces ($N_{xy} = 0$)

[2]In absolute value

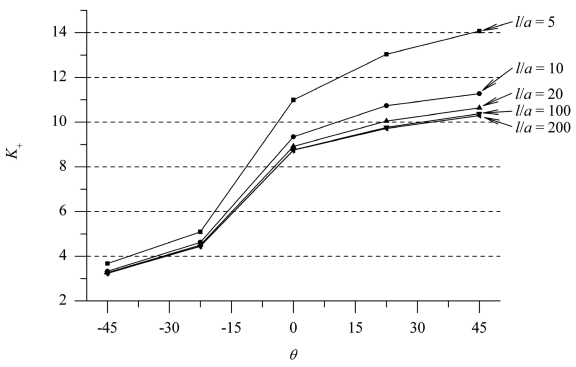

Fig. 9 K_+ vs. θ curves for different values of l/a, and when $N_{xy}/N = 1$

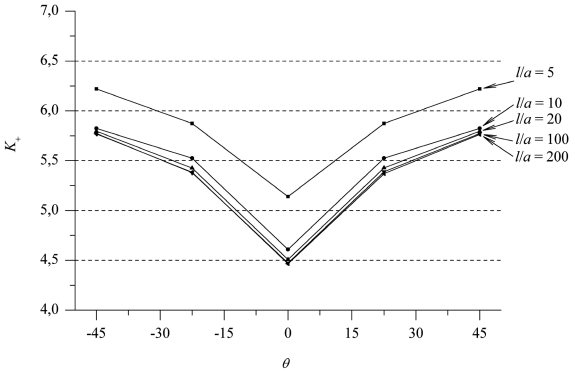

Fig. 10 K_+ vs. θ curves for different values of l/a, and no shear forces ($N_{xy} = 0$)

Table 7 S.C.F for a perforated square plate of different relations l/a and orientation of elastic axes, θ, subjected to pure shear forces (graphite/epoxy)

a/l	θ^o	K_+	β_+	K_-	β_-
0.2	-45,0	4,17	135,00	-22,00	45,00
	-22,5	6,55	120,09	-20,08	51,76
	0,0	17,00	121,28	-17,00	58,72
	22,5	20,07	128,24	-6,55	59,91
	45,0	22,00	135,00	-4,17	45,00
0.1	-45,0	3,67	135,36	-16,73	45,00
	-22,5	5,97	119,92	-15,95	51,59
	0,0	14,23	121,45	-14,23	58,55
	22,5	15,95	128,41	-5,97	60,08
	45,0	16,73	135,00	-3,67	45,00
0.05	-45,0	3,57	135,00	-15,48	45,00
	-22,5	5,76	119,92	-14,68	51,59
	0,0	13,49	121,45	-13,48	58,55
	22,5	14,68	128,41	-5,75	60,08
	45,0	15,48	135,00	-3,57	45,00
0.01	-45,0	3,54	135,36	-14,95	45,00
	-22,5	5,68	119,92	-14,14	51,59
	0,0	13,20	121,45	-13,25	58,55
	22,5	14,14	128,41	-5,68	60,08
	45,0	14,98	135,00	-3,53	45,00
0.005	-45,0	3,52	135,00	-14,84	45,00
	-22,5	5,67	119,92	-14,06	51,59
	0,0	13,19	121,45	-13,15	58,55
	22,5	14,08	128,41	-5,67	60,08
	45,0	14,82	135,00	-3,52	45,00

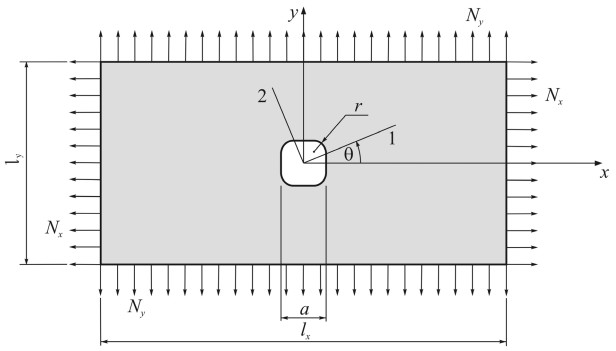

Fig. 11 Rectangular orthotropic plate with a centered square hole under biaxial tension

Table 8 S.C.F for the rectangular perforated plate subjected to biaxial tension (graphite/epoxy)

N_x/N_y	θ^o	K_+	β_+	K_-	β_-
0.5	0,0	3,45	90,00*	-3,25	90,00
	22,5	4,39	132,68	-3,29	123,42
	45,0	7,07	137,32	-0,79	125,77
	67,5	10,72	143,35	-	-
	90,0	9,52	30,85	-	-
2	0,0	5,86	58,98	-	-
	22,5	6,34	126,56	-	-
	45,0	5,69	132,68	-0,29	143,88
	67,5	4,41	138,30	-1,70	147,44
	90,0	3,08	38,59	-2,21	0,00

On the other hand, Figs. 9 and 10 show the variation of K_+, for different values of N_{xy}/N and a/l and two particular values of $\theta = -45^o$ and 45^o.

The case of pure shear forces acting on the outer edge of a square plate with a centered square hole of rounded corners is presented in Table 7.

Finally, a rectangular finite plate $l_x/l_y = 2$, $a/l_y = 0.2$ subjected to biaxial tension is considered (Fig. 11) for two relations of $N_x/N_y = 0.5$ and 2.

Due to the configuration of the loading the azimuthal angle θ was varied from 0^o to 90^o.

Table 8 exhibits the obtained values.

An explanation must be done about the value of K_+ in the first row of Table 8.

For this situation ($N_x/N_y = 0.5$, $\theta = 0^o$) the maximum tension occurs at the outer edges parallel to the coordinate axe x, (which coincide with the constitutive direction 1), at coordinates: $x = 0$, $y = \pm l_y/2$.

The nearness between hole and outer edge cause this behavior.

In this case, the maximum stress concentration factor at the contour of the hole is 3.08 . Certainly, four points symmetrically located ($\beta = 45.89^o$, 134.11^o, 225.89^o and 314.11^o) support this tension.

This situation is shown clearly in Fig. 12.

It is important to point out that for biaxial tension, compressive stresses arise

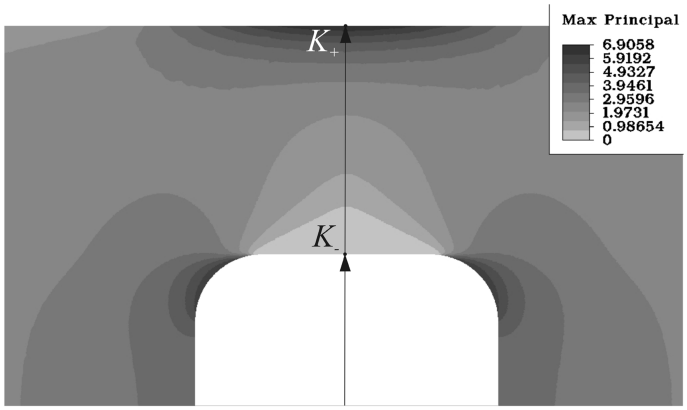

Fig. 12 Stress distribution on the rectangular perforated graphite/epoxy plate for $N_x/N_y = 0.5$ and $\theta = 0^o$

5. Conclusions

The static problem of a laminate graphite/epoxy with a square hole of rounded corners under in-plane loading has been considered by means of a finite element code.

The procedure has been verified in the case of classical solutions of orthotropic plates available in the open literature.

Numerical investigation was performed to demonstrate that for hole size to plate dimension ratios a/l smaller than 0.005 the plate may be considered infinite.

As a general behavior one may conclude that as it occurs in the case of isotropic, linearly elastic solids, K_+ increases as the parameter a/l does. For the orthotropic material investigated, the absolute value of K_-, when arises, also increase, as a/l is incremented.

On the other hand, the values of β_+ and β_- remain practically constant.

Since for tensile loads N_x and N_y, large compressive stresses are originated (Table 8), it seems reasonable to expect for these situations and depending upon the thickness of the plate, localized buckling or wrinkling phenomena.

Extensive and detailed experimental studies are needed in this area.

Acknowledgements

The present study has been sponsored by CONICET Research and Development Program, ANCPYT and by Secretaría General de Ciencia y Tecnología of Universidad Nacional del Sur.

References

ALGOR. Professional Mech/VE (2007), Aslgor Inc., Pittsbourgh, PA. USA.

Amer, M.S. and Schadler, L.S. (1997), "Stress concentration phenomenom in graphite/epoxy composites: Tension/compression effects", *Compos. Sci. Technol.*, **57**, 1129-1137.

Hufenbach, W., Schaffer, M. and Herrmann, A.S. (1990), "Calculation of the stress and displacement field of

anisotropic plates with elliptical hole", *Ingenieur Arch*., **60**, 507-517.
Hüsnü, M.D. and Alaattin, A. (2000), "Analytical and finite element comparisons of stress intensitivy factors of composite materials", *Compos. Struct.,* **50**, 99-102.
Kirsch, G. (1898), Die Theorie der Elasizität und die Bedürfnisee der Festigkeitslehre, Zeit Verem *Deutsch Ing* **42**, 797-807.
Lekhnitskii, S.G. (1968), *Anisotropic Plates*. Gordon & Breach, New York.
Maiz, S., Rossi, R.E., Laura, P.A.A. and Bambill, D.V. (2004), "Efectos de la ortotropía sobre el factor de concentración de tensiones: extensión del problema de Kirsch" (In Spanish). ENIEF 2004 Congress (Bariloche, Argentina). *Mecánica Computacional* **XXIII**, 673-692.
Park, K.H. and Kim, F.J. (2006), "Analytical solution for a circular opening in an elastic-brittle-plastic rock", *Int. J. Rock Mech. Mining Sci.*, **43**, 616-622.
Pilkey, W.D. (1997), *Peterson's Stress Concentration Factors*, John Wiley & Sons, Inc. New York.
Rezaeepazhand, J. and Jafari, M. (2005), "Stress analysis of perforated composite plates", *Compos. Struct.,* **71**, 463-468.
Sharan, S.K. (2008), "Analytical solutions for stresses and displacements around a circular opening in a generalized Hoek-Brown rock", *Int. J. Rock Mech. Mining Sci.,* **45**(1), 78-85.
Susca, A., Bambill, D.V., Laura, P.A.A. and Rossi, R. (2006), "Factor de Concentración de tensiones en el entorno de un orificio rectangular presente en una placa ortótropa", (in spanish) ENIEF 2006 Congress (Santa Fe, Argentina). *Mecánica Computacional* **XXV**, 411-427.
Toubal, L., Karama, M. and Lorrain, B. (2005), "Stress concentration in a circular hole in composite plate", *Compos. Struct.,* **68**, 31-36.
Ukadgaonker, V.G. and Awasare, P.J. (1994), "A novel method of stress analysis of an infinite anisotropic plate with elliptical hole or crack with uniform tensile stress", *J. Inst. Eng.,* **75**, 53-55.
Wu, H. and Mu, B. (2003), "On stress concentration for isotropic/orthotropic plates and cylinders with a circular hole", *Compos. Part B Eng.,* **34**, 127-134.